



ANL/RERTR/TM-2

Dr. 2865
ANL/RERTR/TM-2

120
7-27-81


B 6005 

MASTER

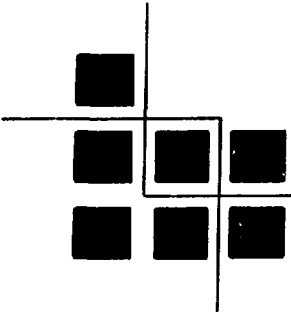
**A STUDY OF UO₂ WAFER FUEL
FOR VERY HIGH-POWER RESEARCH REACTORS**

by

**T. C. Hsieh, V. Z. Jankus,
J. Rest, and M. C. Billone**

BASE TECHNOLOGY

**REDUCED ENRICHMENT
RESEARCH AND TEST REACTOR
PROGRAM**



ARGONNE NATIONAL LABORATORY, ARGONNE, ILL.

DISTRIBUTION OF THIS DOCUMENT IS UNLIMITED

Prepared for the U. S. DEPARTMENT OF ENERGY
Assistant Secretary for Energy Technology
Office of Nuclear Power Development Division
under Contract W-31-109-Eng-38



ANL/RERTR/TM-2

ARGONNE NATIONAL LABORATORY
9700 South Cass Avenue
Argonne, Illinois 60439

A STUDY OF UO_2 WAFER FUEL
FOR VERY HIGH-POWER RESEARCH REACTORS

by

T. C. Hsieh,* V. Z. Jankus,
J. Rest, and M. C. Billone**

Materials Science Division

DISCLAIMER

This document contains information which is proprietary to the United States Government. It is being disseminated to the public for their information only. It is not to be used for any other purpose without the express written permission of the United States Government. The Government makes no warranty, expressed or implied, and assumes no responsibility for the accuracy, completeness, or usefulness of the information contained herein. It is advised that users of this information consult the appropriate technical manuals and standards for the proper use of this information.

November 1980

* Present Address: EG&G Idaho, Inc., Idaho Falls, Idaho 83401
**Present Address: Department of Mechanical and Nuclear Engineering,
Northwestern University, Evanston, Illinois 60201

104

TABLE OF CONTENTS

	<u>Page</u>
ABSTRACT.....	1
I. INTRODUCTION.....	1
II. CAMEL FUEL DESIGN FOR THE OSIRIS REACTOR.....	2
III. CODE DEVELOPMENT AND VERIFICATION.....	5
IV. INVESTIGATIONS OF UO ₂ WAFER FUEL PERFORMANCE.....	14
V. SUMMARY AND CONCLUSIONS.....	25
REFERENCES.....	27

LIST OF FIGURES

<u>No.</u>	<u>Title</u>	<u>Page</u>
1.	Schematic Representations of Cladding and Fuel Components for Compartmented Plate-type Oxide Fuel Elements. (a) Caramel fuel for the Osiris reactor; (b) fuel element for the Shippingport reactor.....	3
2.	Schematic of Thin Plate-type Fuel and Cladding.....	5
3.	Schematic of Hollow Cylindrical Fuel and Cladding.....	6
4.	Fuel Temperature Distributions in a Thin Plate and a Thin Cylindrical Shell.....	8
5.	(a) A Thin Plate of Thickness $2c$; (b) Cross Section of a Thin Cylindrical Shell with $r_i = a$ and $r_o = b$	9
6.	Fuel Centerline Temperature vs Burnup for Four Caramel Fuel Designs.....	21
7.	Fuel Failure Curves for Four Caramel Fuel Designs.....	21
8.	Fuel Centerline Temperature for the 1.45-mm Wafer Design.....	21
9.	Fuel Failure Curve for the 1.45-mm Wafer Design.....	21
10.	Fuel Failure Curve for a 1.50-mm Wafer Under High Coolant Pressure.....	24
11.	Fuel Failure Curve for a 1.50-mm Wafer at a High Cladding Surface Temperature.....	24
12.	Fuel Failure Curve for a 1.50-mm Wafer Under Power-cycling Conditions.....	25

LIST OF TABLES

<u>No.</u>	<u>Title</u>	<u>Page</u>
I.	Design Parameters and Operating Conditions for Caramel Fuel as Used in the Osiris Reactor.....	4
II.	As-Built Data and Irradiation Conditions for Five Plate Samples in NRX Reactor.....	15
III.	LIFE-PLATE Predictions for Five Plate Fuel Samples.....	16
IV.	Fuel Plenum Volume, Fuel Density, and Initial Fuel Porosity for Four Failed Plate Samples.....	17
V.	Fuel Deformations Predicted by LIFE-PLATE for Five Plate Samples.....	17
VI.	Design Parameters for French Caramel Fuel Irradiated in Osiris Reactor.....	18-19
VII.	Maximum Fuel Power Attainable at Two Different Goal Burnups for Various Wafer Designs.....	23

A STUDY OF UO_2 WAFER FUEL
FOR VERY HIGH-POWER RESEARCH REACTORS

by

T. C. Hsieh, V. Z. Jankus, J. Rest and M. C. Billone

ABSTRACT

The Reduced Enrichment Research and Test Reactor Program is aimed at reducing fuel enrichment to $< 20\%$ in those research and test reactors presently using highly enriched uranium fuel. UO_2 caramel fuel is one of the most promising new types of reduced-enrichment fuel for use in research reactors with very high power density. Parametric studies have been carried out to determine the maximum specific power attainable without significant fission-gas release for UO_2 wafers ranging from 0.75 to 1.50 mm in thickness.

The results indicate that (1) all the fuel designs considered in this study are predicted not to fail under full-power operation up to a burnup of 1.09×10^{21} fis/cm³; (2) for all fuel designs, failure is predicted at approximately the same fuel centerline temperature for a given burnup; (3) the thinner the wafer, the wider the margin for fuel specific power between normal operation and increased-power operation leading to fuel failure; (4) increasing the coolant pressure in the reactor core could improve fuel performance by maintaining the fuel at a higher power level without failure for a given burnup; and (5) for a given power level, fuel failure will occur earlier at a higher cladding surface temperature and/or under power-cycling conditions.

I. INTRODUCTION

As part of the U. S. effort on proliferation resistance of fuels and fuel cycles, the Reduced Enrichment Research and Test Reactor (RERTR) Program¹ is aimed at reducing fuel enrichment to less than 20% in those research and test reactors presently using highly enriched uranium fuel. Generally, the enrichment reduction can be accomplished by increasing the total uranium loading of the fuel and/or by increasing the fuel volume fraction through element redesign. The candidate fuels for research and test reactors under this program² include $UAl-Al$ dispersion fuel, U_3O_8-Al dispersion fuel, U_3Si-Al fuel, and UO_2 fuel. The first two of these are current research reactor fuels with fuel loadings $\sim 1.2-1.7$ g U/cm³, but with the potential for development of higher uranium loadings. U_3Si-Al and UO_2 are new types of fuel which provide the enrichment-reduction potential for research reactors with very high power density (VHPD). In France, the CEA fuel development program aimed at reducing proliferation potential in research reactors has

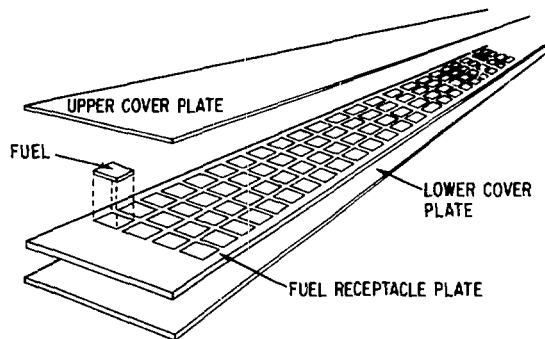
concentrated on UO₂ caramel fuel, with U-Mo alloys as a backup fuel. The French have successfully irradiated UO₂ test wafers, arranged in Zircaloy separators and cladding³ in the 70-MW Osiris reactor, to a burnup of 7.26×10^{20} fis/cm³ (30,000 Mwd/T).

In VHPD research reactors, the fuel centerline temperature must not approach a level at which a significant amount of fission gas is released from the fuel: The accumulation of released fission gas can push the cladding outward to form a fuel-cladding gas gap, thus causing a degradation of the heat transfer across the gap and subsequent higher fuel temperatures. These effects can eventually lead to fuel blistering and cladding breach. Owing to its poor thermal conductivity, UO₂ wafer fuel must be fabricated in the form of thin (<1.5-mm) plates to maintain a sufficiently low centerline temperature. The specific limitations on UO₂ wafer thickness, which vary with research reactor type and irradiation conditions, in turn limit the specific power of the fuel. The purpose of the present report is to provide a description of the development of a production code for UO₂ plate fuel and to report the results of parametric studies performed to establish the operating limits for UO₂ wafer fuel in VHPD research reactors. Based on the available information on the French caramel fuel design and the operating conditions in the Osiris reactor, parametric studies have been carried out to determine the maximum fuel specific power possible before significant fission-gas release occurs (causing the formation of a fuel-cladding gap) for UO₂ wafer thicknesses of 1.50, 1.45, 1.25, 1.00 and 0.75 mm. In the following section, French caramel fuel design for the Osiris reactor will be described. In Section III, a description of the development of a fuel modeling code for UO₂ plate fuel and subsequent code verification will be given. The results of parametric studies are given and discussed in Section IV, and conclusions are presented in Section V.

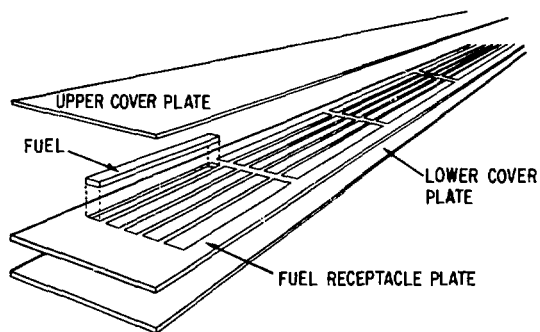
II. CARAMEL FUEL DESIGN FOR THE OSIRIS REACTOR

The French Osiris reactor is a pool-type reactor that used MTR-type 93% enriched UAl fuel elements before conversion to caramel fuel in 1979. The reactor first achieved criticality in 1966 and operated at the initial design power of 50 MW. The operating power was raised to 70 MW in 1968 with the introduction of advanced UAl fuel elements.⁴ The UAl fuel elements were made of 24 flat plates with fuel meat dimensions of 0.508 x 68.55 x 600 mm and a fuel loading of 16.3 g ²³⁵U per plate. The coolant flow rate and coolant pressure at the core inlet were 4,250 m³/h and 107.6 kPa (15.6 psi), respectively.

The French caramel fuel design uses UO₂ fuel (density of 10.25 g/cm³) and Zircaloy cladding in a plate form. The ²³⁵U enrichment is less than 10%. The thickness of the UO₂ fuel ranges from 4 mm for very low-power reactors and critical experiments to 1.45 mm for VHPD research reactors. For the 70-MW Osiris reactor, the caramel fuel design utilizes UO₂ wafers in a compartmentalized Zircaloy cladding arrangement (Fig. 1a). The wafer dimensions are 1.45 x 17.1 x 17.1 mm and the maximum fuel enrichment is 7%.⁵ The caramel fuel design is similar to that employed in the second core of the Shippingport reactor (Fig. 1b), which used UO₂-ZrO₂ as fuel and UO₂ in the blanket.⁶ For complete replacement of UAl fuel by caramel fuel in the Osiris reactor, the coolant flow rate was increased by 30% (from 4,250 to 5,700 m³/h) and the core volume was increased from 30 to 42 assemblies. Table I shows the design parameters of the caramel fuel elements and the operating conditions in the Osiris reactor.



(a)



(b)

Fig. 1. Schematic Representations of Cladding and Fuel Components for Compartmented Plate-type Oxide Fuel Elements. (a) Caramel fuel for the Osiris reactor; (b) fuel element for the Shippingport reactor.

Table I

Design Parameters and Operating Conditions for Caramel Fuel
as Used in the Osiris Reactor

Total number of standard/control assemblies	36/6
Number of plates per standard/control element	17/14
Overall plate length, cm	67.5
Plate thickness, cm	0.225
Active fuel length, cm	58.14
Active fuel width, cm	6.84
Active fuel thickness, cm	0.145
Cladding thickness, cm	0.04
Water-channel thickness, cm	0.2456
Average heat flux, W/cm ²	126.45
Peak heat flux, W/cm ²	323.5
Total heat-transfer area, m ²	56.13
Axial peaking factor	1.3
Radial peak-to-average power factor	1.968
Velocity in coolant channel, m/s	12.54
Coolant inlet temp. (max.), °C	41
Peak coolant temp. rise, °C	27
Core temp. rise, °C	10
Coolant pressure at core inlet, psi	15.64
Peak specific power, W/cm ³	4400

III. CODE DEVELOPMENT AND VERIFICATION

The thermal and mechanical behavior of the UO_2 plate was analyzed by means of a computer code, LIFE-PLATE, generated from an existing production code, LIFE-LWR⁷, which was developed for cylindrical fuel under Light Water Reactor (LWR) operating conditions. The idea is to mathematically map the plate fuel into a thin, hollow cylindrical fuel with appropriate boundary conditions to achieve similarity in thermal and mechanical behavior between plate fuel and cylindrical fuel. In a plate fuel of dimensions $2S \times W \times L$ (Fig. 2), the temperature distribution can be expressed as

$$T_p(x) = T_m - \frac{q'''}{2k_f} x^2 \quad (1)$$

where

T_m = fuel centerline temperature,

k_f = fuel thermal conductivity, assumed constant,

q''' = fuel specific power,

and

x = distance from fuel centerline.

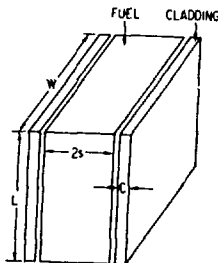


Fig. 2. Schematic of Thin Plate-type Fuel and Cladding.

With the same fuel material and irradiation conditions, the temperature distribution of a hollow, cylindrical fuel (Fig. 3) with inner radius, outer radius, and thickness r_i , r_o and S , respectively, is (again assuming constant k_f) given by

$$T_r(r) = T_m - \frac{q''' r_i^2}{4k_f} \left[\left(\frac{r}{r_i} \right)^2 - 2 \ln \frac{r}{r_i} - 1 \right]. \quad (2)$$

Note that T_m is the temperature at the inner cylinder surface, and no heat flow inward, i.e., into the center of the cylinder is allowed.

Substituting $r = r_i + x$ into Eq. (2) results in

$$T_r'(x) = T_m - \frac{q''' r_i^2}{4k_f} \left[\left(\frac{r_i + x}{r_i} \right)^2 - 2 \ln \frac{r_i + x}{r_i} - 1 \right]. \quad (3)$$

The constant thermal conductivity, volumetric heat rating, outer surface temperature, and cylindrical thickness of the fuel, given by

$$k_f = 0.0252 \text{ W/cm}^\circ\text{K},$$

$$q''' = 4552 \text{ W/cm}^3,$$

$$T(S) = 786.3 \text{ }^\circ\text{C},$$

and

$$S = 0.076 \text{ cm},$$

are used to compare Eqs. (1) and (3).

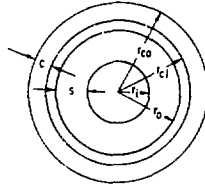


Fig. 3. Schematic of Hollow Cylindrical Fuel and Cladding.

The fuel temperature distributions given by Eqs. (1) and (3) are shown in Fig. 4. In Fig. 4, the solid line represents the plate fuel temperature, the dotted line represents the cylindrical fuel temperature with $r_i = 10S$, and the dashed line represents the cylindrical fuel temperature with $r_i = 50S$. As shown in Fig. 4, with r_i equal to 50 times the half-thickness of the plate fuel and with the same fuel outer surface temperature, the fuel temperature distribution in the cylindrical fuel is almost identical with that of the plate fuel; the maximum temperature difference, at the fuel centerline, is quite small (<0.3%). For a plate cladding of dimensions $C \times W \times L$ (Fig. 2) and a constant cladding thermal conductivity k_c , the temperature distribution in the cladding can be expressed as

$$T_p(x) = T_i - \frac{q''' S x}{k_c}, \quad (4)$$

where

$$T_i = \text{cladding inner surface temperature,}$$

- q''' = fuel specific power,
 S = half thickness of the plate fuel,
 x = outward distance from the cladding inner surface,

and

- k_c = thermal conductivity of the cladding.

Similarly, the temperature distribution in a cylindrical cladding (Fig. 3) is

$$T_r(r) = T_i - \frac{q''' \frac{(r_o^2 - r_i^2)}{2} \ln \frac{r}{r_{ci}}}{k_c} \quad (5)$$

or

$$T_r'(x) = T_i - \frac{q''' \frac{(r_o^2 - r_i^2)}{2} \ln \frac{r_{ci} + x}{r_{ci}}}{k_c}, \quad (6)$$

where

- r_o = fuel outer radius,
 r_i = fuel inner radius,
 r_{ci} = cladding inner radius,

and

- r_{co} = cladding outer radius.

Given practical values of

- q''' = 4552 W/cm³,
 k_c = 0.164 W/cm-°K,
 r_i = 3.80 cm,
 r_o = 3.876 cm,
 r_{ci} = 3.886 cm,
 r_{co} = 3.946 cm,

$$S = r_o - r_i = 0.076 \text{ cm,}$$

$$T_o = (\text{cladding outer surface temperature}) = 130^\circ\text{C,}$$

and

$$C = r_{co} - r_{ci} = 0.06 \text{ cm,}$$

one may calculate

$$T_i = 130 + \frac{4552 \cdot 0.076 \cdot 0.06}{0.1642} = 256.4 \quad (\text{plate});$$

$$T_i = 130 + \frac{4552 \cdot \frac{3.876^2 - 3.8^2}{2} \ln \frac{3.946}{3.886}}{0.1642} = 253.9^\circ\text{C} \quad (\text{cylinder}).$$

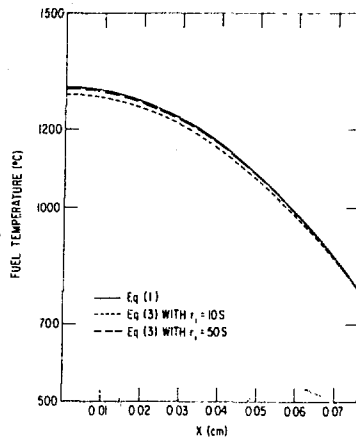


Fig. 4. Fuel Temperature Distributions in a Thin Plate and a Thin Cylindrical Shell.

Again, the cladding temperature distribution for the cylindrical geometry is almost identical with that of the plate cladding; the maximum temperature difference (at the cladding inner surface) is very small (<1.0%). Therefore, the use of cylindrical geometry for representation of a flat plate is valid in terms of the temperature distribution in both fuel and cladding, as long as the inner radius of the cylindrical fuel is chosen to be 50 times larger than the half-thickness of the plate fuel.

For the mechanical analysis, the thin-slab thermoelastic solution was compared with the thin-tube solution with regard to maximum tensile stress (at fuel and cladding outer surface) and maximum compressive stress (at fuel and cladding inner surface) to show the adequacy of employing a cylindrical geometry for representation of a flat plate.

For a thin slab of thickness $2c$ (Fig. 5a), the following assumptions are made:

- (a) Plane stress, i.e., $\sigma_{zz} = 0$.
- (b) $\sigma_{xy} = \sigma_{yz} = \sigma_{zx} = 0$.
- (c) Temperature distribution in the slab is a function of z only; i.e., $T = T(z)$.
- (d) $\sigma_{xx} = f(z)$ and $\sigma_{yy} = f(z)$.
- (e) The edges of the plate are perfectly restrained against expansion and rotation; i.e., $\epsilon_{xx} = \epsilon_{yy} = 0$.
- (f) Constant thermoelastic properties.

The thermoelastic solution is obtained from the stress-strain relationship as

$$\sigma(z) = \frac{\bar{E} \bar{\alpha}}{1 - \bar{\nu}} \left[-T(z) + \frac{1}{2c} \int_{-c}^c T(z) dz \right]. \quad (7)$$

For the thin shell (Fig. 5b), the thermoelastic solution⁸ is given by

$$\sigma_{\theta}(r) = \frac{\bar{E} \bar{\alpha}}{1 - \bar{\nu}} \left[-T(r) + \frac{1 + a^2/r^2}{1 - a^2/b^2} \frac{1}{b^2} \int_a^b T(r) r dr + \frac{1}{r^2} \int_a^r T(r) r dr \right], \quad (8)$$

where

a = the inner radius of the thin shell,

b = the outer radius of the thin shell,

and

\bar{E} , $\bar{\alpha}$, $\bar{\nu}$ = constants.

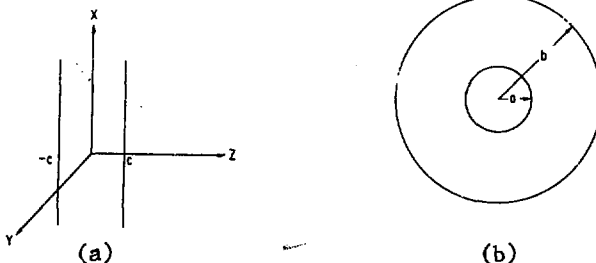


Fig. 5. (a) A Thin Plate of Thickness $2c$; (b) Cross Section of a Thin Cylindrical Shell with $r_i = a$ and $r_o = b$.

For fuel and cladding with $\frac{dT}{dz}$ and $\frac{dT}{dr} < 0$, the maximum tensile stress occurs at $z = c$ and $r = b$ for the slab and shell geometries, respectively. A linear temperature distribution in the cladding region is assumed for simplicity, i.e.,

$$T(z) = T_o + \frac{\Delta T(c - z)}{2c} \quad (\text{slab}) \quad (9)$$

and

$$T(r) = T_o + \frac{\Delta T(b - r)}{b - a} \quad (\text{shell}). \quad (10)$$

Substituting the above temperatures into Eqs. (7) and (8),

$$\sigma(c) = 1/2 \frac{\bar{E}\bar{\alpha}\Delta T}{1 - \bar{\nu}} \quad (11)$$

and

$$\sigma_{\theta}(b) = \frac{\bar{E}\bar{\alpha}\Delta T}{1 - \bar{\nu}} \frac{b + 2a}{3(b + a)} \quad (12)$$

for maximum tensile stress, and

$$\sigma(-c) = -1/2 \frac{\bar{E}\bar{\alpha}\Delta T}{1 - \bar{\nu}} \quad (13)$$

and

$$\sigma_{\theta}(a) = -\frac{\bar{E}\bar{\alpha}\Delta T}{1 - \bar{\nu}} \frac{a + 2b}{3(b + a)} \quad (14)$$

for maximum compressive stress.

As the thickness of the wall ($b - a$) becomes small in comparison with the outer radius (b) of the cylinder, i.e., $b/a \rightarrow 1$, it can be shown that

$$\sigma_{\theta}(b) = 1/2 \frac{\bar{E}\bar{\alpha}\Delta T}{1 - \bar{\nu}} = \sigma(c) \quad (15)$$

and

$$\sigma_{\theta}(a) = -1/2 \frac{\bar{E}\bar{\alpha}\Delta T}{1 - \bar{\nu}} = \sigma(-c) \quad (16)$$

In order to evaluate the thermal stresses in the plate and thin shell for the case where $b/a \neq 1$, consider $a = 5.156$ cm and $b = 5.207$ cm.

From Eqs. (12) and (14), it is seen that

$$\sigma_{\theta}(b) = 0.499 \frac{\bar{E}\bar{\alpha}\Delta T}{1-\nu} \quad (17)$$

and

$$\sigma_{\theta}(a) = -0.501 \frac{\bar{E}\bar{\alpha}\Delta T}{1-\nu} \quad (18)$$

Equations (17) and (18) are almost identical with Eqs. (15) and (16). Therefore, assuming a linear temperature distribution in the cladding for plate and cylindrical geometries, the distribution of thermal stresses over the thickness of the wall for a cylindrical shell is almost identical with that for a flat plate of thickness $2c = b - a$.

For fuel, a quadratic temperature distribution is assumed:

$$T(z) = T_o + \Delta T \left[1 - \left(\frac{z}{c} \right)^2 \right] \quad (19)$$

and

$$T(r) = T_o + \Delta T \left[1 - \frac{(r-a)^2}{(b-a)^2} \right]. \quad (20)$$

Substituting these temperatures into Eqs. (7) and (8), it is seen that

$$\sigma(c) = \frac{2}{3} \frac{\bar{E}\bar{\alpha}}{1-\nu} \Delta T \quad (21)$$

and

$$\sigma_{\theta}(b) = \frac{\bar{E}\bar{\alpha}\Delta T}{1-\nu} \left[1 - \frac{1}{6} \frac{(3b+a)}{(b+a)} \right] \quad (22)$$

for maximum tensile stress, and

$$\sigma(-c) = -\frac{1}{3} \frac{\bar{E}\bar{\alpha}}{1-\nu} \Delta T \quad (23)$$

and

$$\sigma_{\theta}(a) = \frac{\bar{E}\bar{\alpha}\Delta T}{1-\nu} \frac{1}{6} \left[\frac{(3b+a)}{(b+a)} \right] \quad (24)$$

for maximum compressive stress.

Again, with $b/a \rightarrow 1$, it is found that

$$\sigma_{\theta}(b) \rightarrow \frac{2}{3} \frac{\bar{E}\bar{\alpha}}{1 - \bar{\nu}} = \sigma(c) \quad (25)$$

and

$$\sigma_{\theta}(a) - \frac{1}{3} \frac{\bar{E}\bar{\alpha}\Delta T}{1 - \bar{\nu}} = \sigma(-c). \quad (26)$$

In order to evaluate the thermal stresses in the plate and thin shell for the case where $b/a \neq 1$, consider

$$a = 5.080 \text{ cm}$$

and

$$b = 5.156 \text{ cm.}$$

These values lead to

$$\sigma_{\theta}(b) = 0.665 \frac{\bar{E}\bar{\alpha}\Delta T}{1 - \bar{\nu}} \quad (27)$$

and

$$\sigma_{\theta}(a) = -0.335 \frac{\bar{E}\bar{\alpha}\Delta T}{1 - \bar{\nu}}. \quad (28)$$

These calculations indicate that the maximum tensile and compressive stresses of a cylindrical-shell fuel region are almost the same as those of a flat-plate fuel region, assuming a quadratic temperature distribution in the fuel. Furthermore, the distribution of thermal stresses over the thickness of the wall for a cylindrical fuel is almost identical with the case of plate fuel of thickness $2c = b - a$, since the temperature distribution over the thickness of the wall is identical in the two cases.

LIFE-PLATE is an integral fuel-modeling code that has been generated for UO_2 plate fuel irradiated under normal operation conditions (i.e., start-up, steady power, slow power changes and shutdown). The code is based on LIFE-LWR, which is an LWR fuel-rod performance code for UO_2 fuel and Zr cladding. A number of modifications have been made in LIFE-LWR to generate LIFE-PLATE. These include the following:

- (a) A code option has been added which allows the cladding outer surface temperature to be specified as an input to the code. The cladding surface temperature input to the code can be obtained from a simplified hand calculation or from a sophisticated thermal-hydraulics code.

- (b) A mechanistic gas release and swelling code, FASTGRASS,⁹ has been coupled to LIFE-PLATE to predict the fission-gas behavior in the fuel. The approach of coupling FASTGRASS to LIFE-PLATE is similar to that used in an experimental version of LIFE-LWR developed by Rest.¹⁰ After the operating conditions, such as fuel dimensions, local fuel temperatures and stresses, grain size, fuel densities, and linear power are calculated in LIFE-PLATE, the FASTGRASS subroutine calculates the bubble radii for the various size classes of bubbles; the bubble diffusivities, mobilities, and coalescence probabilities; and the bubble diffusion and migration rates. Then FASTGRASS solves for the bubble size distributions and calculates the amount of fission gas released and retained, as well as the fuel swelling strain due to retained fission gas. For plate wafer fuel, the amount of gas released from the fuel is crucial in deciding whether the fuel will fail or not. Therefore, a fundamental and reliable gas release and swelling code should be used.
- (c) A boundary condition, which assumes that the pressure at the inner surface of the fuel (corresponding to the midplane of the plate fuel) is the same as the pressure of the coolant at the outer surface of the cladding, has been added to LIFE-PLATE. This assumption is based on the plane stress approximation to treat a flat plate. Practically, this boundary condition prevents cylindrical fuel and cladding, which are in intimate contact under steady-power operation before fuel failure, from creeping either inward or outward.
- (d) The code is modified such that fission gas is not permitted to enter the central hole of the cylindrical fuel. However, fission gas released from the fuel is allowed to go into a hollow cylindrical plenum located at the top of the fuel, with radius as large as the inner radius of the cladding. Plenum size is specified according to the experimental observations of the fission gas release necessary to start the blistering and is treated in the code as a calibration parameter.
- (e) During the opening of the fuel-cladding gap, caused by the accumulation of fission gas in the plenum, the plenum pressure is permitted to vary only within $\pm 3\%$ of its value from the previous time step in order to eliminate numerical oscillations of the code (due to the small plenum in the UO₂ wafer fuel).

LIFE-PLATE has been tested numerically using various coolant-pressure, fuel-radius, fuel-cladding gap conductance, and fuel-length values to debug and streamline the code. LIFE-PLATE predictions have been compared with results of plate irradiation experiments which were conducted in the NRX reactor at Chalk River in 1960 by Westinghouse,¹¹ to ensure that the code is predicting reasonable fuel deformations and fission-gas releases. The irradiation program was part of the development of the UO₂ plates for the blanket employed in the second core of the Shippingport reactor. About 200 UO₂ wafer samples (including about 30 plates that had failed during irradiation) were irradiated. They covered a wide range of fuel densities (88-99% TD), fuel enrichments (3.8-63.7%), fuel widths (0.318-1.27 cm), fuel wafer thicknesses (0.76-4.06 mm), irradiation temperatures (254-324°C) at cladding OD, and fuel burnups (0.5-15.0 at. %).

Table II shows the as-fabricated data and irradiation conditions in the NRX reactor for five plate samples, M42-1C, M31-1C, 4H2-1A, 6H2-1A, and 2L2-1A. Each test element contained six or twelve fuel wafers (Fig. 1a) and was assembled, seal welded, evacuated, and then bonded at 843°C for 4 hours under a helium pressure of 69 MPa (10,000 psi) without deliberate incorporation of a void volume. Table III shows LIFE-PLATE predictions of fission-gas release and fuel centerline temperature at the beginning of life for the five plate samples. Since neither the contact conductance of UO₂-Zircaloy interfaces nor the contact pressures were known accurately, the above calculations were performed by assuming a constant gap conductance of 0.625 W/cm²°C. As shown in Table IV, fair agreement between measured and calculated fission-gas release was obtained. Fuel failures were observed in test plates M42-2C, M31-1D, 2H1-2C and 1H2-2A.

Based on the power history of the test samples, the plenum volume was adjusted in the code so that the opening of the fuel-cladding gap (taken as the onset of fuel blistering here) predicted by LIFE-PLATE would be in agreement with the experimental observations. Table IV shows plenum volumes, fuel densities, and initial fuel porosities for test samples M42-2C, M31-1D, 2H1-2C and 1H2-2A. The plenum volume is very close to the initial fuel porosity in each failed plate. With plenum volumes equal to the initial fuel porosities, LIFE-PLATE predicted no fuel failures for test runs 4H2 and 2L2, in agreement with experimental data. Therefore, the plenum volume was set equal to the initial fuel porosity in the code.

The fuel deformations predicted by LIFE-PLATE have also been qualitatively compared with the experimental data for plate samples M42-1C, M31-1C, 4H2-1A, 6H2-1A, and 2L2-1A (Table V). For each test element, the measurements were made at several positions and only the average value was reported, while LIFE-PLATE predictions are for the maximum fuel deformation at the center of the plate. As shown in Table V, the predictions made by LIFE-PLATE agree fairly well with the experimental data.

IV. INVESTIGATIONS OF UO₂ WAFER FUEL PERFORMANCE

Parametric studies with UO₂ wafer thickness ranging from 0.75 to 1.50 mm were conducted for caramel fuel irradiated in the Osiris reactor to determine the maximum specific power at which significant fission-gas release and gap opening would occur. The fuel design is taken from Ref. 3 and the design parameters are listed in Table VI. Owing to limited information on French caramel fuel design and operating conditions in the Osiris reactor, most data in Table VI are our best guesses. Table VI gives the possible design parameters for 0.75, 1.00, 1.25 and 1.50-mm-thick fuel wafers. In these designs, the cladding thickness, reactor core size and power, and coolant mass flow rate are kept the same. The fuel enrichment has been increased for thin wafer designs to compensate for the decrease in fuel volume fraction. The parametric studies are based on the data listed in Table VI, which differ from those of Table I; however, at the end of this section, it will be shown that the domain of these parametric studies actually included the design case given in Table I. The studies were based on the following assumptions:

Table II

As-built Data and Irradiation Conditions for Five Plate Samples in NRX Reactor

	Fuel Sample				
	<u>M42-1C</u>	<u>M31-1C</u>	<u>4H2-1A</u>	<u>6H2-1A</u>	<u>2L2-1A</u>
Width, ^a cm	0.635	0.635	0.635	0.318	0.635
²³⁵ U Enrichment, wt%	52.1	52.1	52.0	63.7	55.4
Fuel Density, % TD	88	97	97	97	87
Cladding Thickness, cm	0.051	0.051	0.051	0.051	0.051
Coolant Pressure, psi	2000	2000	2000	2000	2000
Average Heat Flux, W/cm ²	167.2	179.8	201.9	186.1	173.5
Burnup, at. %	14.89	7.88	7.45	13.58	7.88

^aAll samples were 3.81 cm long and 0.102 cm thick.

Table III

LIFE-PLATE Predictions for Five Plate Fuel Samples

<u>Fuel Sample</u>	<u>Burnup, at.%</u>	<u>Fission Gas Released, % Th</u>		<u>Fuel Centerline Temp. BOL, °F</u>
		<u>Measured</u>	<u>Calculated</u>	
M42-1C	14.89	14.1	8.38	1708
M31-1C	7.88	3.7	3.75	1657
UH2-1A	7.44	2.8	4.50	1695
6G2-1A	13.58	7.8	6.84	1680
2L2-1A	7.88	4.1	6.32	1828

Table IV

Fuel Plenum Volume, Fuel Density, and Initial Fuel Porosity
for Four Failed Plate Samples

<u>Test Plate</u>	<u>Plenum Volume, percent of fuel volume</u>	<u>Fuel Density, % TD</u>	<u>Initial Fuel Porosity, %</u>
M42-2C	12.3	88	12
M31-1D	1.7	97	3
1H2-2A	2.7	97	3
2H1-2C	2.7	96.4	3.6

Table V

Fuel Deformations Predicted by LIFE-PLATE for Five Plate Samples

<u>Fuel Sample</u>	<u>Burnup, at.%</u>	<u>Δt (mils)</u>	
		<u>Measured (average)</u>	<u>Calculated</u>
M42-1C	15.81	2.1	3.64
M31-1C	7.59	2.1	3.08
4H2-1A	7.17	1.5	2.1
6H2-1A	13.08	4.1	3.94
2L2-1A	8.47	2.0	3.0

Table VI

Design Parameters^a for French Caramel Fuel Irradiated in
Osiris Reactor

	Wafer Thickness, mm			
	0.75	1.00	1.25	1.50
No. of fuel plates per fuel element	20	18	17	16
Plate thickness, mm	1.77	2.02	2.27	2.52
Active fuel thickness, mm	0.75	1.00	1.25	1.50
Water channel thickness, mm	2.35	2.56	2.58	2.63
Average heat flux, W/cm ²	115.74	128.60	136.17	144.68
Total heat transfer area, m ²	60.48	54.43	51.41	48.38
Velocity in coolant channel, m/s	10.31	10.48	11.1	11.47
Peak specific power, W/cm ³ oxide	7283	6070	5060	4552
Fuel enrichment, %	11.2	9.4	8	7

^aThe following design parameters are the same for all four wafer designs:

Total no. of fuel assemblies -	45	Core temp. rise, °C -	25.1
No. of wafers per plate -	84	Coolant pressure at core inlet, psi -	15.64
Active fuel length, cm -	56	Fast neutron flux, avg/max -	1.94/ 4.16x10 ¹⁴
Clad thickness, mm -	0.51	Thermal neutron flux, avg/max -	0.85/2x10 ¹⁴
Radial peak-to-average power factor -	2.36	Fuel density, % TD -	93.5

- (a) The fabrication processes for French caramel fuel are the same as those for elements of the x-1-p and x-3-m tests, which included test samples of M42-1C, M31-1C, 4H2-1A, 6H2-1A, and 2L2-1A: i.e., fuel platelets that were sintered at 1750°C, coated with 0.356-1.02 μm of pyrolytic carbon by cracking methane at 1030°C and isostatically pressure bonded without deliberate incorporation of any void volume.
- (b) Before fuel-cladding gap opening, the gap conductance has a constant value of 0.625 $\text{W}/\text{cm}^2\text{°C}$, and the plenum volume is 6.5% of total fuel volume.
- (c) A constant water film coefficient of 4.54 $\text{W}/\text{cm}^2\text{°C}$ can be used in the cladding OD temperature calculations.
- (d) There is no heat transfer through fuel-cladding interfaces in the thickness-length plane (i.e., ribs).

For each fuel wafer design, the performance of the hottest wafer was analyzed by using LIFE-PLATE. Figure 6 shows the centerline temperatures of the peak power wafers irradiated in the Osiris reactor vs fuel burnups of up to 1.09×10^{21} fis/cm^3 (45,000 MWd/T) and for wafer thicknesses of 1.50, 1.25, 1.00, and 0.75 mm. As shown in Fig. 6, the thinner the wafer, the lower the calculated fuel centerline temperature. By varying the specific power of the UO_2 fuel in each wafer design (assuming cladding OD temperature and irradiation conditions remain the same), LIFE-PLATE predicts the time at which the fuel-cladding gap starts to form as a result of the internal pressure arising from the accumulation of fission gas released from the fuel. In LIFE-PLATE, when plenum pressure exceeds fuel-cladding interfacial pressure by one percent, a gap between fuel and cladding is allowed to form. The opening of the gap will cause degradation in the fuel-cladding heat transfer and will lead to high fuel temperature. These processes will lead to fuel blistering and cladding failure. Therefore, for a conservative approach, the opening of the gap can be regarded as the onset of fuel blistering and fuel failure. The curve of fuel specific power vs time of fuel failure (as described above) is defined here as the fuel failure curve. Figure 7 shows the fuel failure curves for 1.50, 1.25, 1.00, and 0.75-mm-thick fuel designs.

In order to clarify the meaning of the fuel failure curves in Fig. 7, we will consider the following example for a 1.50-mm-thick wafer design. Under full power, the peak specific power (which is used here to mean fuel power per unit volume of oxide fuel) of the fuel wafer is 4552 W/cm^3 and LIFE-PLATE predicts that there is no gap between fuel and cladding up to a burnup of 1.09×10^{21} fis/cm^3 (45,000 MWd/T). However, if the fuel specific power were raised to 5462 W/cm^3 , LIFE-PLATE would predict fuel failure at a burnup of 6.29×10^{20} fis/cm^3 (26,000 MWd/T) and thus generate a point on the fuel failure curve (Fig. 7).

Figures 8 and 9 show the fuel centerline temperature under full-power conditions and the fuel failure curve, respectively, for the standard

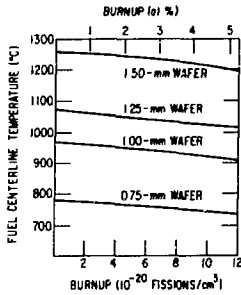


Fig. 6. Fuel Centerline Temperature vs Burnup for Four Caramel Fuel Designs.

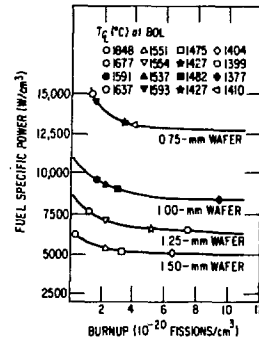


Fig. 7. Fuel Failure Curves for Four Caramel Fuel Designs.

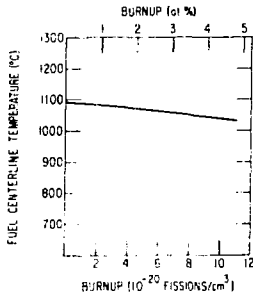


Fig. 8. Fuel Centerline Temperature for the 1.45-mm Wafer Design.

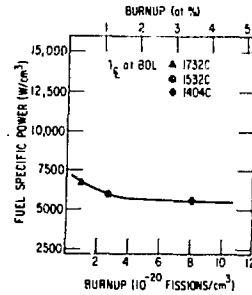


Fig. 9. Fuel Failure Curve for the 1.45-mm Wafer Design.

(1.45-mm-thick) caramel wafer design according to the data listed in Table I. Comparing Fig. 8 with Fig. 6, one sees that the fuel centerline temperature of 1.50-mm-thick fuel (data taken from Ref. 3) is about 167°C higher than that of 1.45-mm-thick fuel (data taken from Ref. 5). This is due mainly to the lower average heat flux and thinner cladding of the fuel in the 1.45-mm fuel design. The following observations can be made: (a) All of the fuel wafer designs considered are predicted not to fail under full-power operations up to a burnup of 1.09×10^{21} fis/cm³ (45,000 MWd/t). (b) For each fuel design and a given initial fuel temperature, the fuel is predicted to fail at approximately the same burnup (Fig. 7). (c) The thinner the wafer, the larger the margin that exists for fuel specific power between normal operation and increased-power operation leading to fuel failure. (d) For the same goal burnup, the thinnest wafer design has the shortest residence time in the core. This conclusion is based on the assumption that the cladding thicknesses and reactor core sizes are the same in all four wafer designs. The increases in fuel enrichment, which are required in thin wafer designs to compensate for

the decrease in fuel volume fraction in the core and to reach criticality, cause the decrease of fuel residence time for a given goal burnup. If the fabrication technology allows the cladding thicknesses to be varied in proportion to wafer thicknesses, e.g., a cladding thickness of 0.51 mm for a 1.50-mm wafer design and a cladding thickness of 0.26 mm for a 0.75-mm wafer design, then

$$q'' \text{ (0.75-mm wafer)} = \frac{1}{2} q'' \text{ (1.50-mm wafer)}$$

and

$$\begin{aligned} q''' \text{ (0.75-mm wafer)} &= \frac{2 q'' \text{ (0.75-mm wafer)}}{0.75} = \frac{2 q'' \text{ (1.50-mm wafer)}}{1.50} \\ &= q''' \text{ (1.50-mm wafer)} \end{aligned}$$

where

$$q'' = \text{heat flow rate of fuel per unit area}$$

and

$$q''' = \text{fuel specific power.}$$

Thus, the fuel specific powers and fuel enrichments are the same in all four wafer designs (neglecting flux depression), and fuel residence time would be the same to a given burnup. Table VII shows the maximum specific power each wafer design can reach before fuel failure for the goal burnups of 7.26×10^{20} and 1.09×10^{21} fis/cm³ (30,000 and 45,000 MWd/T). The fuel centerline temperature at each fuel power level at the beginning of life is also included. The values of peak specific power listed in Table VII can be interpreted as follows: Under steady reactor power conditions similar to that of the Osiris reactor, if the peak fuel specific power was increased to 4,940, 5,350, 6,440, 8,500, and 12,600 W/cm³ for the 1.50, 1.45, 1.25, 1.00 and 0.75-mm wafer designs, respectively (through increases in fuel enrichment), the wafer designs could be used in the research reactors with powers of 76, 85, 89, 98, and 123 MW, respectively, to a fuel burnup of 1.09×10^{21} fis/cm³ (45,000 MWd/T) without fuel failure. Under the above reactor powers, the fuel centerline temperatures at the beginning of life for all five wafer designs are about the same ($\sim 1400^\circ\text{C}$). The fuel residence time for peak-power wafers is 93.4, 86.2, 71.6, 54.3, and 36.6 days for the 1.50, 1.45, 1.25, 1.00, and 0.75-mm wafer designs, respectively.

Fuel failure could conceivably be affected by factors such as coolant pressure, cladding temperature, and power cycling. Figure 10 shows the fuel failure curve for the 1.50-mm wafer design under similar operating conditions in the Osiris reactor with a coolant pressure of 6.9 MPa (i.e., a much larger coolant pressure than used in the previous calculations). The maximum specific power a fuel wafer can sustain is 5,460 and 5,280 W/cm³ for burnups of 7.26×10^{20} and 1.09×10^{21} fis/cm³ (30,000 & 45,000 MWd/T), respectively, about 10% higher than that listed in Table VII. The higher coolant pressure exerted on the cladding surface will make the formation of a fuel-cladding gas gap more difficult, i.e., release of more fission gas from the fuel is required to generate a pressure great enough to overcome the coolant pressure and form the

Table VII

Maximum Fuel Power Attainable at Two Different
Goal Burnups for Various Wafer Designs

Wafer Thickness, mm	Goal Burnup, fis/cm ³	Peak Specific Power, W/cm ³ Oxide	Fuel Centerline Temp. BOL, °F
0.75	7.26x10 ²⁰	12,700	2,560
	1.09x10 ²¹	12,600	2,540
1.00	7.26x10 ²⁰	8,620	2,540
	1.09x10 ²¹	8,500	2,500
1.25	7.26x10 ²⁰	6,470	2,560
	1.09x10 ²¹	6,470	2,500
1.45	7.26x10 ²⁰	5,540	2,570
	1.09x10 ²¹	5,350	2,480
1.50	7.26x10 ²⁰	4,980	2,550
	1.09x10 ²¹	4,940	2,520

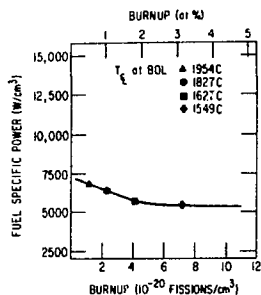


Fig. 10. Fuel Failure Curve for a 1.50-mm Wafer Under High Coolant Pressure.

gas gap. Therefore, for a given fuel specific power, the effect of higher coolant pressure is to prolong the time to fuel failure and, for a given fuel burnup, the effect of higher coolant pressure is that the fuel can operate at a higher power level.

If the fuel wafer were irradiated with a higher cladding temperature, one would expect a higher fuel centerline temperature [from Eq. (1), the fuel surface temperature is higher] and release of a larger amount of fission gas from the fuel for the same power level. This effect is shown in Fig. 11, which gives results for a 1.50-mm wafer irradiated with a cladding temperature of 260°C. The fuel is predicted to fail at a burnup of $\sim 1.7 \times 10^{20}$ fis/cm³ at a fuel power of 5,240 W/cm³.

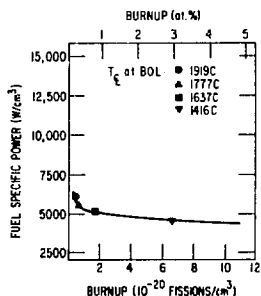


Fig. 11. Fuel Failure Curve for a 1.50-mm Wafer at a High Cladding Surface Temperature.

Figure 12 shows the fuel failure curve for a 1.50-mm wafer irradiated in the Osiris reactor under power-cycling conditions. The reactor power is assumed to start up and shut down every 200 hours. For a very high fuel specific power (say, 5,500 W/cm³), the power-cycling effect is not prominent because the fuel fails before the end of one or two power cycles. Therefore,

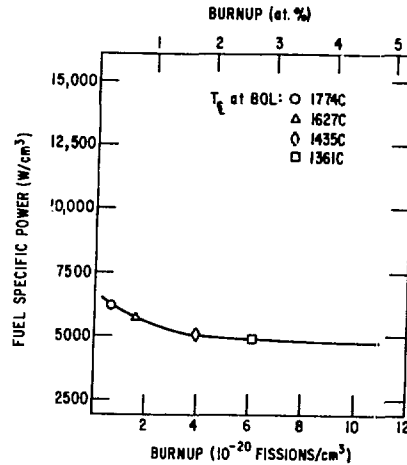


Fig. 12. Fuel Failure Curve for a 1.50-mm Wafer Under Power-cycling Conditions.

there is no significant difference between Figs. 7 and 12 with respect to the high-power regions of the 1.50-mm fuel failure curves. At a fuel specific power of 5,010 W/cm³, power-cycling conditions and steady-power operation will result in fuel failure at burnups of 4.84×10^{20} and 6.05×10^{20} fis/cm³ (20,000 and 25,000 MWd/T), respectively. Here, the earlier fuel failure for the power-cycling case is due to the larger fuel deformations and greater amount of gas release from the fuel.

V. SUMMARY AND CONCLUSIONS

The potential for conversion of any reactor to reduced-enrichment fuel generally depends on the reactor type, the current uranium density in the fuel, and the power density, and must be assessed on an individual basis. The evaluation of the fuel design depends on the fuel-cycle cost and fuel performance. An economical fuel-cycle cost requires thick plates separated by wide water channels. High fuel performance, on the other hand, is achieved with thin plates and narrow water gaps. The proposed compromise will depend on the characteristics of each reactor. LIFE-PLATE analysis of the French caramel fuel, which is designed specifically for the Osiris reactor, indicated that the goal burnup of 1.09×10^{21} fis/cm³ (45,000 MWd/T) will be reached without fuel failure by the peak-power wafer under full-power conditions for 1.50, 1.45, 1.25, 1.00, and 0.75-mm wafer designs. At the indicated goal burnup, these designs would allow a maximum specific power of 4940, 5350, 6440, 8550, and 12,600 W/cm³, respectively. The thinner the wafer, the larger the margin that exists for fuel specific power between normal operation and increased-power operation leading to fuel failure. Thin wafers provide the potential for fuel conversion for even high-power (>70 MW) research reactors. Very high fuel performance can be achieved with a fuel design that uses thin wafers as well as thin cladding. Increasing the coolant pressure in the reactor core could improve the fuel performance, by maintaining the fuel at a higher power level without failure for a given burnup. Fuel failure will occur earlier for a given power level at a

higher cladding surface temperature and/or under power-cycling conditions.

The new fuel types considered for conversion of very high-power research reactors include U_3Si , U-Mo alloys, and UO_2 fuel, which are all in the form of flat plates. With modifications in descriptions of fission-gas release and swelling and substitution of appropriate thermal and mechanical parameters, LIFE-PLATE will be capable of analyzing fuel performance of U_3Si and U-Mo fuels under normal reactor operating conditions. Furthermore, fuel behavior under reactor transient conditions can also be predicted by LIFE-PLATE with some code modifications which have already been employed in LIFE-4T¹², a combined steady-state and transient fuel performance code for LMFBR fuel.

REFERENCES

1. J. E. Matos, *RERTR Program Generic Studies*, Trans. Am. Nucl. Soc. 32 Suppl. 1, 31 (1979).
2. D. Stahl, *The Status and Development Potential of Plate-Type Fuels for Research and Test Reactors*, Argonne National Laboratory Report ANL-79-11 (March 1979).
3. J. P. Schwartz, *Uranium Dioxide Caramel Fuel*, presented at International Conference on Nuclear Non-Proliferation and Safeguards, AIF, New York, Oct. 22-25, 1978.
4. J. Bernot and B. Lerouge, *Osiris: Operation and Utilization Status*, presented at CEA-CONF-1462, CEA, Saclay, France (Dec. 1969).
5. J. P. Schwartz, *Combustible Caramel Pour Reacteurs De Recherche*, presented at International Conference on Nuclear Non-Proliferation and Safeguards, New York (October 1978).
6. M. L. Bleiberg, R. M. Berman, and B. Lustman, *Effects of High Burn-Up on Oxide Ceramic Fuels*, in *Radiation Damage in Reactor Materials*, IAEA, Vienna, 1963, pp. 319-428.
7. *Light-Water-Reactor Safety Research Program - Quarterly Progress Report*, July-September, 1976, Argonne National Laboratory Report, ANL-76-121, p. 48-61.
8. S. Timoshenko and J. N. Goodier, *Theory of Elasticity*, 3rd Ed., McGraw-Hill, p. 448 (1970).
9. J. Rest and S. Gehl, *The Mechanistic Prediction of Fission-Gas Behavior During In-Cell Transient Heating Tests on LWR Fuel Using the GRASS-SST and FASTGRASS Computer Codes*, Trans. 5th Intl. Conf. on Structural Mechanics in Reactor Technology, Berlin, W. Germany, Aug. 13-17, 1979, T. A. Jaeger and B. A. Boley, Eds. North-Holland Publ. Co., 1979, Vol. C, paper C 1/6.
10. J. Rest, *SST: A computer Code to Predict Fuel Response and Fission Product Release From Light-Water Reactor Fuels During Steady-State and Transient Conditions*, Trans. Am. Nucl. Soc. 22, 462 (1975).
11. R. C. Daniel, M. L. Bleiberg, H. B. Meieran, and W. Yeniscavich, *Effects of High Burnup on Zircaloy-Clad, Bulk UO₂, Plate Fuel Element Samples*, Bettis Atomic Power Laboratory Report WARD-263 (Sept. 1962).
12. Y. Y. Liu, *LIFE4/4T Coupling*, presented at LIFE Working Group Meeting, Richland, WA, September 28, 1979.